Inorganic Chemistry

Article

pubs.acs.org/IC

Design of Triads for Probing the Direct Through Space Energy Transfers in Closely Spaced Assemblies

Jean-Michel Camus,[†] Shawkat M. Aly,[‡,§] Daniel Fortin,[‡] Roger Guilard,*[,†] and Pierre D. Harvey*[,†,‡]

[†]Institut de Chimie Moléculaire de l'Université de Bourgogne (ICMUB, UMR 6302), Université de Bourgogne, UFR Sciences et Techniques, 9 Avenue Alain Savary, BP 47870, 21078 Dijon, France

[‡]Département de Chimie, Université de Sherbrooke, 2500 Boulevard de l'Université, Sherbrooke, Quebec, Canada J1K 2R1

Supporting Information

ABSTRACT: Using a selective stepwise Suzuki cross-coupling reaction, two trimers built on three different chromophores were prepared. These trimers exhibit a **D**^**A**$_1$-**A**$_2$ structure where the donor **D** (octa-β-alkyl zinc(II)porphyrin either as diethylhexamethyl, **10a**, or tetraethyltetramethyl, **10b**, derivatives) through space transfers the S_1 energy to two different acceptors, di(4-ethylbenzene) zinc(II)porphyrin (**A**$_1$; acceptor 1) placed cofacial with **D**, and the corresponding free base (**A**$_2$; acceptor 2), which is *meso*−*meso*-linked with **A**$_1$. This structure design allows for the possibility of comparing two series of assemblies, **9a,b** (**D**^**A**$_1$) with **10a,b** (**D**^$\hat{\mathbf{A}}_1$-**A**$_2$), for the evaluation of the S_1 energy transfer for the global process **D***→**A**$_2$ in the trimers. From the comparison of the decays of the fluorescence of **D**, the rates for through space energy transfer, k_{ET} for **10a,b** ($k_{ET} \approx 6.4 \times 10^9$ (**10a**), 5.9×10^9 s^{-1} (**10b**)), and those for the corresponding cofacial **D**^**A**$_1$ systems, **9a,b**, ($k_{ET} \approx 5.0 \times 10^9$ (**9a**), 4.7×10^9 s^{-1} (**9b**)), provide an estimate for k_{ET} for the direct through space **D***→**A**$_2$ process (i.e., k_{ET}(**D**^**A**$_1$-**A**$_2$) − k_{ET}(**D**^**A**$_1$) = k_{ET}(**D***→**A**$_2$) ∼ 1×10^9 s^{-1}). This channel of relaxation represents ∼15% of k_{ET} for **D***→**A**$_1$.

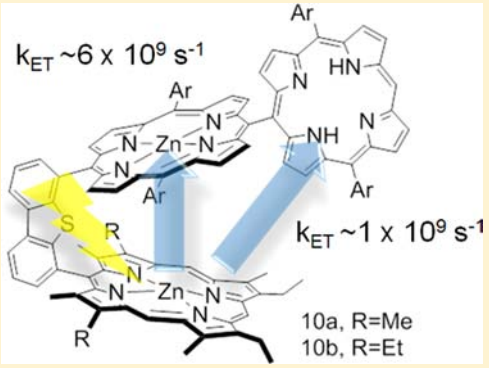

INTRODUCTION

Through space singlet, S_1, energy transfers are among the key processes in the antenna effect in the photosynthetic membranes.[1] In the past decades, large efforts have been devoted to mimic natural photoinduced electron and energy transfers[2,3] and excitation energy migration (exciton).[4] However, these molecular-based models, mostly focusing on multiporphyrin architectures, dyads and multiads, have largely been based on direct covalent or coordination bonds,[2,4] but not exclusively since H-bonding[5] and occasionally electrostatic interactions[2b] as means to assemble porphyrins together have been reported. Consequently in laboratory models, these key photophysical processes unavoidably occur with chemical or H-bonds placed between the donor (**D**) and acceptor (**A**), hence drastically contrasting with the natural systems found in the photosynthesis membranes. These photophysical **D**−**A** events can occur at very short time scale (fs−ps).[6] Conversely, several studies on cofacial **D**^**A** models (^ = bridge), where only through space S_1 energy transfers occur, were reported.[2] To the best of our knowledge, these models for S_1 energy transfers were exclusively limited to dyads bringing the inconvenience that relay effect and cascade events could not be studied. This simplistic situation hinders the understanding of the multiple, not to say complex, events in the natural systems. This work reports two trimer **D**^**A**$_1$-**A**$_2$ systems (**10a,b**; Chart 1) where **D** (octaalkyl zinc(II)porphyrin) can transfer its S_1 energy to two different acceptors, a cofacial diaryl zinc(II)porphyrin (**A**$_1$; acceptor 1) and the corresponding free base (**A**$_2$; acceptor 2) linked to **A**$_1$ via a *meso*−*meso*-bond (Chart 1). By comparing the rates of energy transfers, k_{ET}, with those for the cofacial **D**^**A**$_1$ systems (**9a,b**; Chart 1), k_{ET} for the direct through space S_1 energy transfer **D***→**A**$_2$ is deduced (Figure 1). This channel of relaxation represents ∼15% of k_{ET} for **D***→**A**$_1$.

Chart 1. Structures of 9a,b and 10a,b Showing the Through Space S_1 Energy Transfers (Ar = 4-Ethylbenzene)

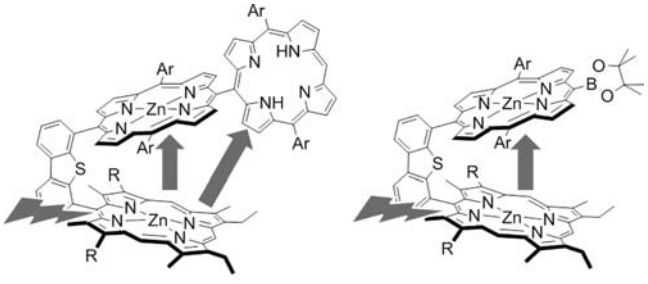

Received: December 5, 2012
Published: July 11, 2013

   dx.doi.org/10.1021/ic3026655 | *Inorg. Chem.* 2013, 52, 8360−8368

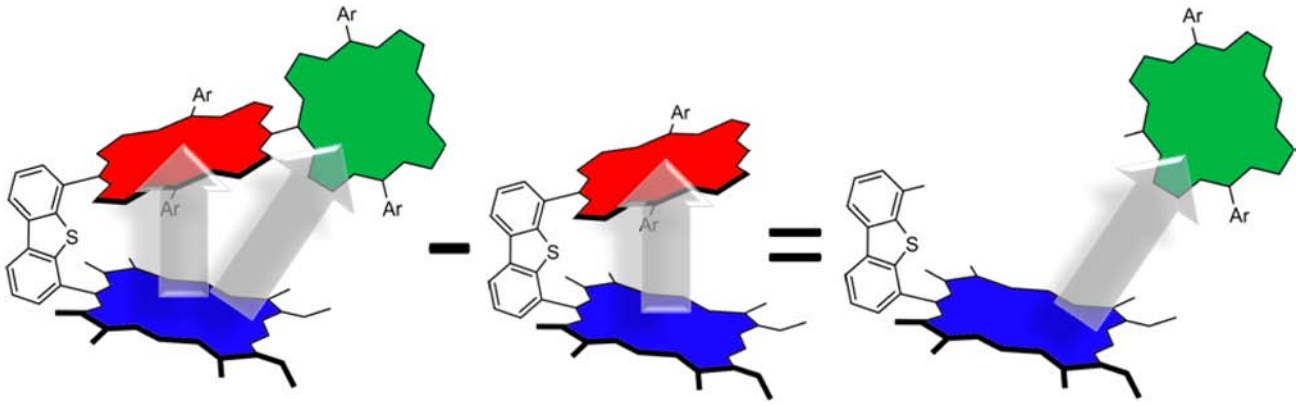

Figure 1. Diagram showing how the k_{ET} for $\mathbf{D}^*\rightarrow\mathbf{A_2}$ is deduced (blue = **D**; red = $\mathbf{A_1}$; green = $\mathbf{A_2}$).

EXPERIMENTAL SECTION

Materials. 4,6-Dibromodibenzothiophene (**1**) and 2,2′-dipyrromethane were synthesized according to the literature.[7,8] The porphyrin precursors a,c-biladienes (**3a**,**b**) were synthesized as previously reported.[9] The handling of all air/water sensitive materials was carried out using standard high vacuum techniques. Dried toluene was obtained by passing through alumina under nitrogen in the solvent purification systems and then further dried over activated molecular sieves; extra dry DMF and 4-ethylbenzaldehyde were purchased from Aldrich. Triethylamine, DCM, and 1,2-dichloroethane were distilled from CaH_2; THF was distilled from sodium benzophenone ketyl. Unless specified otherwise all other solvents were used as commercially supplied. Silica gel (Merck; 70−120 mm) was used for column chromatography. Analytical thin layer chromatography was performed using Merck 60 F254 silica gel (precoated sheets, 0.2 mm thick). Reactions were monitored by thin-layer chromatography, UV−vis spectroscopy, and MALDI/TOF mass spectrometry. Size exclusion chromatography was carried out under gravity using cross-linked polystyrene Bio-Beads SX-1 (200 − 400 mesh) in DCM. The ^{1}H NMR and mass spectra are placed in the Supporting Information (SI).

*4-Bromo-6-formyldibenzothiophene (**2**).* A 3.2 g portion of of 4,6-dibromodibenzothiophene (**1**) (9.3 mmol) was dissolved in 120 mL of anhydrous THF, and the solution was cooled down to −78 °C. PhLi (4.9 mL, 9.8 mmol) was added dropwise, and the reaction mixture was stirred one hour at low temperature. A 5 mL portion of anhydrous DMF was added at −78 °C, and the reaction mixture was allowed to warm to room temperature while stirring for 2 h. The reaction was quenched with water and diluted with 100 mL of CH_2Cl_2. The organic phase was washed with a saturated aqueous NH_4Cl solution, washed with brine, and dried over $MgSO_4$. The solution was concentrated *in vacuo*, and crystallization at −30 °C afforded **2** as a light yellow powder (2.10 g, 78%). ^{1}H NMR (300.16 MHz, $CDCl_3$): δ 10.29 (s, 1H, CHO), 8.38 (dd, 1H, J = 7.9 Hz, J = 0.8 Hz), 8.15 (dd, 1H, J = 7.9 Hz, J = 0.8 Hz), 8.02 (dd, 1H, J = 8.0 Hz, J = 1.0 Hz), 7.70 (t, 1H, J = 7.7 Hz), 7.65 (dd, 1H, J = 7.7 Hz, J = 1.0 Hz), 7.39 (t, 1H, J = 7.8 Hz) ppm. ^{13}C NMR (75.47 MHz, $CDCl_3$): δ 191.3, 143.5, 137.9 (2C), 135.0, 133.4, 130.9, 130.2, 127.7, 126.3, 125.0, 120.4, 116.8 ppm. ESI MS m/z: 312.9310 $[M + Na]^+$, 312.9293 calcd for $C_{13}H_7BrNaOS$.

*Zinc(II) 5-(4-(Bromodibenzothien-6-yl))-(13,17-diethyl-2,3,7,8,12,18-hexamethyl)porphyrin (**4a**).* A mixture of a,c-biladiene dihydrobromide (**3a**) (0.95 g, 1.5 mmol) and 4-bromo-6-formyldibenzothiophene (**2**) (0.44 g, 1.5 mmol) in 150 mL of absolute ethanol was deoxygenated by bubbling argon for 15 min and heated under reflux conditions. A solution of p-toluenesulfonic acid (2.0 g, 10.6 mmol) in 100 mL of degassed ethanol was added dropwise over 10 h, and the reaction mixture was stirred overnight under reflux. After cooling down the reaction mixture to room temperature, the volatiles were removed under vacuum, and the residue was dissolved in CH_2Cl_2, washed with a saturated $NaHCO_3$ aqueous solution, and washed with brine. The organic phase was dried over $MgSO_4$ and was concentrated *in vacuo*. A saturated methanolic (10 mL) solution of $Zn(OAc_2)\cdot 2H_2O$ was added. The mixture was stirred overnight and washed with brine. The organic layer was dried over $MgSO_4$ and evaporated until dryness. Purification by successive silica gel chromatographic columns (dichloromethane/pentane 1/2 and THF/pentane 5/100) afforded the product as a brick red powder (0.28 g, yield 23%). ^{1}H NMR (300.16 MHz, THF-d_8): δ 10.16 (s, 2H, *meso*), 10.09 (s, 1H, *meso*), 8.68 (dd, 1H, J = 1.1 Hz, J = 7.8 Hz, thiophene), 8.50 (dd, 1H, J = 1.1 Hz, J = 7.8 Hz, thiophene), 8.18 (dd, 1H, J = 1.1 Hz, J = 7.6 Hz, thiophene), 7.99 (dt, 1H, J = 7.7 Hz, thiophene), 7.58 (dd, 1H, J = 1.1 Hz, J = 7.6 Hz, thiophene), 7.47 (t, 1H, J = 7.7 Hz, thiophene), 4.14 (q, 2H, J = 7.5 Hz, CH_2), 4.13 (q, 2H, J = 7.5 Hz, CH_2), 3.65 (s, 6H, CH_3), 3.48 (s, 6H, CH_3), 2.27 (s, 6H, CH_3), and 1.91 (t, 6H, J = 7.5 Hz, CH_3) ppm. ESI HRMS m/z: 772.1208 $[M]^{\bullet+}$, 772.1160 calcd for $C_{42}H_{37}BrN_4SZn$. UV−vis (THF) λ_{max} (log ε) = 411 (5.53), 541 (4.25), 577 (4.18).

*Zinc(II) 5-(4-(Bromodibenzothien-6-yl))-(2,8,13,17-tetraethyl-3,7,12,18-tetramethyl)porphyrin (**4b**).* This was synthesized by using a,c-biladiene dihydrobromide (**3b**) (1.75 g, 2.9 mmol) and following the above procedure. The compound was isolated as a red brick powder (0.60 g, yield 27%). ^{1}H NMR (300.16 MHz, THF-d_8): δ 10.17 (s, 2H, *meso*), 10.07 (s, 1H, *meso*), 8.70 (d, 1H, J = 8.0 Hz, thiophene), 8.58 (d, 1H, J = 7.2 Hz, thiophene), 8.49 (d, 1H, J = 7.9 Hz, thiophene), 7.97 (t, 1H, J = 7.6 Hz, thiophene), 7.54 (d, 1H, J = 7.9 Hz, thiophene), 7.45 (t, 1H, J = 8.0 Hz, thiophene), 4.14 (q, 2H, J = 7.5 Hz, CH_2), 4.13 (q, 2H, J = 7.5 Hz, CH_2), 3.65 (s, 6H, CH_3), 3.52 (s, 6H, CH_3), 2.88 (q, 2H, J = 7.4 Hz, CH_2), 2.32 (m, 2H, CH_2), 1.91 (t, 6H, J = 7.4 Hz, CH_3), and 1.04 (t, 6H, J = 7.5 Hz, CH_3) ppm. ESI HRMS m/z: 823.1413 $[M + Na]^+$, 823.1419 calcd for $C_{44}H_{41}BrN_4SZnNa$. UV−vis (THF) λ_{max} (log ε) = 412 (5.53), 541 (4.24), 577 (4.18) nm.

*10,20-Bis(4-ethylphenyl)porphyrin (**5**).* Following a published procedure,[10] a solution of 2,2′-dipyrromethane (2.0 g, 14 mmol) and 4-ethylbenzaldehyde (1.7 mL, 14 mmol) in dichloromethane (1.5 L) was flushed with argon for 5 min. The reaction mixture was protected from the light and vigorously stirred. Trifluoroacetic acid (0.72 mL, 9.0 mmol) was added dropwise. After stirring overnight, DDQ (3.18 g, 14.0 mmol) was added in portions, and the mixture was stirred for another 1 h. Triethylamine (1 mL) was added, and the entire reaction mixture was concentrated and filtered through a pad of alumina. The alumina pad was washed with CH_2Cl_2 until the eluent was colorless. Removal of solvent and chromatography over silica gel (CH_2Cl_2/petroleum ether 2/3) afforded a purple solid which was precipitated in a CH_2Cl_2/MeOH medium (2.1 g, 28%). ^{1}H NMR (300.16 MHz, $CDCl_3$): δ 10.29 (s, 2H, *meso*), 9.37 (d, J = 4.6 Hz, 4H, β), 9.10 (d, J = 4.7 Hz, 4H, β), 8.17 (d, J = 7.9 Hz, 4H, Ar), 7.62 (d, J = 8.0 Hz, 4H, Ar), 3.02 (q, J = 7.6 Hz, 4H, CH_2), 1.54 (t, J = 7.6 Hz, 6H, CH_3), and −3.10 (s, 2H, NH) ppm. ^{13}C NMR (75.47 MHz, $CDCl_3$): δ 147.6 (2C), 145.3 (2C), 143.9 (2C), 138.9 (2C), 135.2 (4C), 131.7 (4C), 131.4 (4C), 126.8 (4C), 105.4, 29.1, and 16.1 ppm. ESI HRMS m/z: 519.2529 $[M + H]^+$, 519.2543 calcd for $C_{36}H_{31}N_4$. UV−vis (THF) λ_{max} (log ε) = 405 (5.62), 501 (4.23), 535 (3.80), 576 (3.70), 633 (3.24) nm.

dx.doi.org/10.1021/ic3026655 | *Inorg. Chem.* 2013, 52, 8360−8368

*5-Bromo-10,20-bis(4-ethylphenyl)porphyrin (**6**).* From a standard procedure,[11] a stirred solution of porphyrin **5** (400 mg, 0.77 mmol) in $CHCl_3$ (250 mL) was cooled in an ice bath for 15 min. NBS (120 mg, 0.70 mmol) was added. After stirring for 10 min the reaction was quenched with acetone (20 mL), and the crude product was purified by column chromatography over silica gel (CH_2Cl_2/petroleum ether 1/5). The solution was concentrated, and the product was precipitated as a purple solid upon addition of methanol (0.26 g, 56%). ^{1}H NMR (300.16 MHz, CD_2Cl_2): δ 10.14 (s, 1H, *meso*), 9.69 (d, J = 5.1 Hz, 2H, β), 9.26 (d, J = 5.1 Hz, 2H, β), 8.93 (d, J = 4.6 Hz, 4H, β), 8.06 (d, J = 8.0 Hz, 4H, Ar), 7.58 (d, J = 8.0 Hz, 4H, Ar), 2.96 (q, J = 7.6 Hz, 4H, CH_2), 1.49 (t, J = 7.6 Hz, 6H, CH_3), and −3.11 (s, 2H, NH) ppm. ^{13}C NMR (75.47 MHz, CD_2Cl_2): δ 143.9 (2C), 138.6 (2C), 134.8 (4C), 132.4 (2C), 132.1, 131.9 (2C), 131.8 (2C), 131.5 (2C), 126.4 (4C), 120.4 (2C), 105.5, 103.5, 28.9 (2C), and 15.8 (2C) ppm. ESI HRMS m/z: 619.1416 $[M + Na]^+$, 619.1468 calcd for $C_{36}H_{29}BrN_4Na$. UV−vis (THF) λ_{max} (log ε) = 412 (5.59), 508 (4.20), 542 (3.71), 585 (3.58), 641 (3.54) nm.

*Zinc(II) 5,15-Bis-(4,4,5,5-tetramethyl-1,3,2-dioxaborolan-2-yl)-10,20-bis(4-ethyl-phenyl)porphyrin (**7**).* From a standard procedure,[10] NBS (0.33 g, 1.90 mmol) was added to an ice bath cooled solution of porphyrin **5** (0.45 g, 0.86 mmol) in $CHCl_3$ (300 mL). After stirring for 30 min, the reaction was quenched with acetone (20 mL), and the solution was reduced to a small volume. Methanol was added, and the precipitate was washed with methanol and dried *in vacuo*. The intermediate dibromoporphyrin was suspended in a $CHCl_3$/MeOH (10/1) mixture, and $Zn(OAc_2)\cdot 2H_2O$ was added. The suspension was refluxed for 2 h, and the solvent was concentrated in vacuum. Water was added and the precipitate filtered and washed with water, methanol, and acetone. The resulting powder was dried to give a purple solid. The zinc-metalated porphyrin and *trans*-dichlorobis-(triphenylphosphine)palladium(II) (38 mg, 0.054 mmol) were placed in a Schlenk flask, and the flask was pump-filled with argon three times. Anhydrous 1,2-dichloroethane (80 mL), triethylamine (3.1 mL, 22 mmol), and pinacolborane (2.0 mL, 13.8 mmol) were successively added, and the resulting mixture was stirred under reflux for 30 min. The reaction was cooled to room temperature and quenched with 30% aq. KCl (50 mL). The organic phase was separated, washed with water (100 mL), and dried over $MgSO_4$. The solvent was removed by rotary evaporation, and the residue was then purified by column chromatography (silica gel, CH_2Cl_2/petroleum ether 4/1) to deliver the product as a purple powder (0.55 g, 77% yield). ^{1}H NMR (300.16 MHz, $CDCl_3$): δ 9.93 (d, J = 4.7 Hz, 4H, β), 9.13 (d, J = 4.7 Hz, 4H, β), 8.15 (d, J = 7.9 Hz, 4H, Ar), 7.61 (d, J = 7.9 Hz, 4H, Ar), 3.04 (q, J = 7.6 Hz, 4H, CH_2), 1.86 (s, 24H, CH_3), 1.57 (t, J = 7.6 Hz, 6H, CH_3) ppm. ^{13}C NMR (75.47 MHz, $CDCl_3$): δ 153.4 (4C), 150.4 (4C), 143.5, 140.5, 134.8 (4C), 133.0 (4C), 132.7 (4C), 126.2 (4C), 121.0 (2C), 85.4 (2C), 29.1 (2C), 25.6 (4C), and 16.1 (2C) ppm. HR-MALDI-TOF m/z: 832.3388 $[M]^{\bullet+}$, 832.3326 calcd for $C_{48}H_{50}B_2N_4O_4Zn$. UV−vis (THF) λ_{max} (log ε) = 420 (5.55), 546 (4.13), 581 (3.63) nm.

*Zinc(II) 5-[10,20-Bis-(4-ethylphenyl)porphyrin-5-yl]-15-(4,4,5,5-tetramethyl-[1,3,2]-dioxaborol-an-2-yl)-10,20-(4-ethylphenyl)-porphyrin (**8**).* Under an inert atmosphere, a mixture of **6** (72 mg, 0.12 mmol), **7** (0.14 g, 0.17 mmol), cesium carbonate (0.11 g, 0.34 mmol), $Pd(PPh_3)_4$ (14 mg, 0.012 mmol) in 10 mL of anhydrous toluene, and 5 mL of DMF was stirred at 90 °C for 5 h. The solvents were removed, and the residue was redissolved in toluene (50 mL) and stirred with an aqueous saturated NH_4Cl solution (50 mL). The organic layer was separated and washed with water (2 × 60 mL) and dried over $MgSO_4$. The solvent was evaporated, and purification by column chromatography (silica gel, chloroform/petroleum ether 1/1 to 3/1) afforded the product as a purple solid (90 mg, 62%). ^{1}H NMR (300.16 MHz, CD_2Cl_2): δ 10.37 (s, 1H, *meso*), 9.98 (d, 2H, J = 4.8 Hz, β), 9.46 (d, 2H, J = 4.6 Hz, β), 9.15 (d, 2H, J = 4.7 Hz, β), 9.10 (d, 2H, J = 4.7 Hz, β), 8.69 (d, 2H, J = 4.6 Hz, β), 8.64 (d, 2H, J = 4.8 Hz, β), 8.14 (m, 8H, Ar), 8.09 (d, 2H, J = 4.7 Hz, β), 8.02 (d, 2H, J = 4.8 Hz, β), 7.55 (d, 4H, J = 8.1 Hz, C_6H_4), 7.52 (d, 4H, J = 8.1 Hz, C_6H_4), 2.92 (q, 4H, J = 7.4 Hz, CH_2), 2.91 (q, 4H, J = 7.4 Hz, CH_2), 1.91 (s, 12H, CH_3), 1.44 (t, 6H, J = 7.4 Hz, CH_3), 1.43 (t, 6H, J = 7.4 Hz, CH_3), and −2.42 (s, 2H, NH). ESI HRMS m/z: 1223.4807 $[M + H]^+$, 1223.4856 calcd for $C_{78}H_{68}BN_8O_2Zn$. UV−vis (THF) λ_{max} (log ε) = 418 (5.42), 447 (5.23), 513 (4.49), 559 (4,51), 590 (4.14) 649 (3.47) nm.

*Zinc(II) 5-{4-[Zinc(II)(13,17-diethyl-2,3,7,8,12,18-hexamethyl)-porphyrin-5-yl]-dibenzothien-6-yl}-15-(4,4,5,5-tetramethyl-[1,3,2]-dioxaborolan-2-yl)-10,20-bis-(4-ethylphenyl)porphyrin (**9a**).* Under an inert atmosphere, a mixture of **4a** (50 mg, 0.064 mmol), **7** (81 mg, 0.1 mmol), cesium carbonate (65 mg, 0.2 mmol), $Pd(PPh_3)_4$ (7.4 mg, 0.006 mmol) in 10 mL of distilled toluene, and 5 mL of anhydrous DMF was stirred at 90 °C for 5 h. The reaction mixture was quenched with 10 mL of an aqueous NH_4Cl (20 mL) solution. The organic layer was separated, washed with water (2 × 20 mL), and dried over $MgSO_4$. The solvent was evaporated, and the residue was purified by column chromatography (silica gel, dichloromethane/petroleum ether 1/2 to 3/2) to afford the product as a red-purple powder (58 mg, 65%). ^{1}H NMR (300.16 MHz, CD_2Cl_2): δ 9.79 (s, 2H, *meso*), 9.63 (s, 1H, *meso*), 9.57 (d, 2H, J = 4.7 Hz, β), 8.88 (d, 2H, J = 7.9 Hz, thiophene), 8.76 (d, 2H, J = 4.8 Hz, β), 8.74 (d, 2H, J = 4.7 Hz, β), 8.70 (d, 2H, J = 4.6 Hz, β), 8.24 (d, 1H, J = 7.2 Hz, thiophene), 8.06−7.97 (m, 3H, thiophene), 7.90 (d, 2H, J = 7.6 Hz, C_6H_4), 7.68 (d, 2H, J = 7.6 Hz, C_6H_4), 7.47 (t, 4H, J = 7.6 Hz, C_6H_4), 3.77 (q, 4H, J = 7.6 Hz, CH_2), 3.34 (s, 6H, CH_3), 3.31 (s, 6H, CH_3), 2.96 (q, 4H, J = 7.6 Hz, CH_2), 2.28 (s, 6H, CH_3), 1.66 (s, 12H, CH_3), 1.60 (t, 6H, J = 7.4 Hz, CH_3), and 1.50 (t, 6H, J = 7.4 Hz, CH_3) ppm. ESI HRMS m/z: 1420.4328 $[M + Na]^+$, 1420.4338 calcd for $C_{84}H_{75}BN_8O_2SZn_2Na$. UV−vis (THF) λ_{max} (log ε) = 410 (5.52), 427 (5.36), 546 (4.26), 577 (4.04), 596 (3.59) nm.

*Zinc(II) 5-{4-[Zinc(II)(2,8,13,17-tetraethyl-3,7,12,18-tetramethyl)-porphyrin-5-yl]-dibenzothien-6-yl}-15-(4,4,5,5-tetramethyl-[1,3,2]-dioxaborolan-2-yl)-10,20-bis-(4-ethylphenyl)porphyrin (**9b**).* Following the above procedure, a mixture of **4b** (56 mg, 0.070 mmol), **7** (70 mg, 0.084 mmol), cesium carbonate (55 mg, 0.17 mmol), and $Pd(PPh_3)_4$ (7.4 mg, 0.006 mmol) in 15 mL of anhydrous toluene/DMF solvents (2/1) was stirred at 90 °C for 5 h. The reaction mixture was quenched with 10 mL of water. After a workup similar as described above, a red-purple solid (59 mg, 59%) was obtained. ^{1}H NMR (both isomers, 300.16 MHz, CD_2Cl_2): δ 9.87 (s, 1H, *meso*), 9.85 (s, 3H, *meso*), 9.69 (s, 1H, *meso*), 9.63 (s, 1H, *meso*), 9.58 (d, 1H, J = 4.9 Hz, β), 9.57 (d, 3H, J = 4.9 Hz, β), 8.92 (dd, 1H, J = 0.9 Hz, J = 4.4 Hz, thiophene), 8.89−8.87 (m, 3H, thiophene), 8.77−8.66 (m, 8H, β), 8.64 (d, 4H, J = 0.8 Hz, β), 8.30 (dd, 1H, J = 0.8 Hz, J = 7.5 Hz, thiophene), 8.20 (dd, 1H, J = 1.0 Hz, J = 7.5 Hz, thiophene), 8.18 (dd, 1H, J = 0.8 Hz, J = 7.5 Hz, thiophene), 8.13 (dd, 1H, J = 0.9 Hz, J = 7.5 Hz, thiophene), 8.05−7.97 (m, 4H, thiophene), 7.89 (m, 4H, C_6H_4), 7.67 (d, 4H, J = 7.1 Hz, C_6H_4), 7.47 (m, 8H, C_6H_4), 3.78 (m, 8H, CH_2), 3.41 (s, 3H, CH_3), 3.39 (s, 3H, CH_3), 3.37 (s, 6H, CH_3), 3.36 (s, 6H, CH_3), 2.97 (q, 8H, J = 7.8 Hz, CH_2), 2.72 (q, 4H, J = 7.8 Hz, CH_2), 2.54 (m, 4H, CH_2), 2.26 (s, 3H, CH_3), 1.67 (s, 24H, CH_3), 1.63 (s, 3H, CH_3), 1.60 (t, 9H, J = 7.5 Hz, CH_3), 1.56−1.48 (m, 18H, CH_3), and 1.02 (t, 9H, J = 7.5 Hz, CH_3) ppm. HR-MALDI-TOF m/z: 1426.4745 $[M]^{\bullet+}$, 1426.4730 calcd for $C_{86}H_{79}BN_8O_2SZn_2$. UV−vis (CH_2Cl_2) λ_{max} (log ε) = 405 (5.66), 422 (5.45), 543 (5.45), 573 (5.29) nm. The presence of two conformational isomers was noted, VT ^{1}H NMR measurements were performed to demonstrate this, and molecular modeling was used to find the origin of this effect (SI).

*Zinc(II) 5-{4-[Zinc(II)(13,17-diethyl-2,3,7,8,12,18-hexamethyl)-porphyrin-5-yl]-dibenzothien-6-yl}-[10,20-bis-(4-ethylphenyl)-porphyrin-5-yl]-10,20-bis-(4-ethyl-phenyl)porphyrin (**10a**).* Under an inert atmosphere, a mixture of **9a** (35 mg, 0.025 mmol), **6** (22 mg, 0.037 mmol), cesium carbonate (16 mg, 0.050 mmol), and $Pd(PPh_3)_4$ (3.4 mg, 0.003 mmol) in 15 mL of anhydrous toluene/DMF solvents (2/1) was stirred at 90 °C for 14 h. The reaction mixture was quenched with 10 mL of an aqueous NH_4Cl (20 mL) solution. The organic layer was separated, washed with water (2 × 20 mL), and dried over $MgSO_4$. Purification by column chromatography (silica gel, chloroform/petroleum ether 1/1) followed by preparative size exclusion chromatography (BioRad Bio-Beads SX-1 packed in CH_2Cl_2) afforded the product as a brownish purple solid (22 mg, 48%). ^{1}H NMR (300.16 MHz, CD_2Cl_2): δ 10.29 (s, 1H, *meso*), 9.93 (s, 2H, *meso*), 9.87 (s, 1H, *meso*), 9.40 (d, 1H, J = 4.9 Hz, β), 9.39 (d,

dx.doi.org/10.1021/ic3026655 | *Inorg. Chem.* 2013, 52, 8360−8368

Scheme 1. Synthesis of 10a,b (Ar = 4-C_6H_4Et)[a]

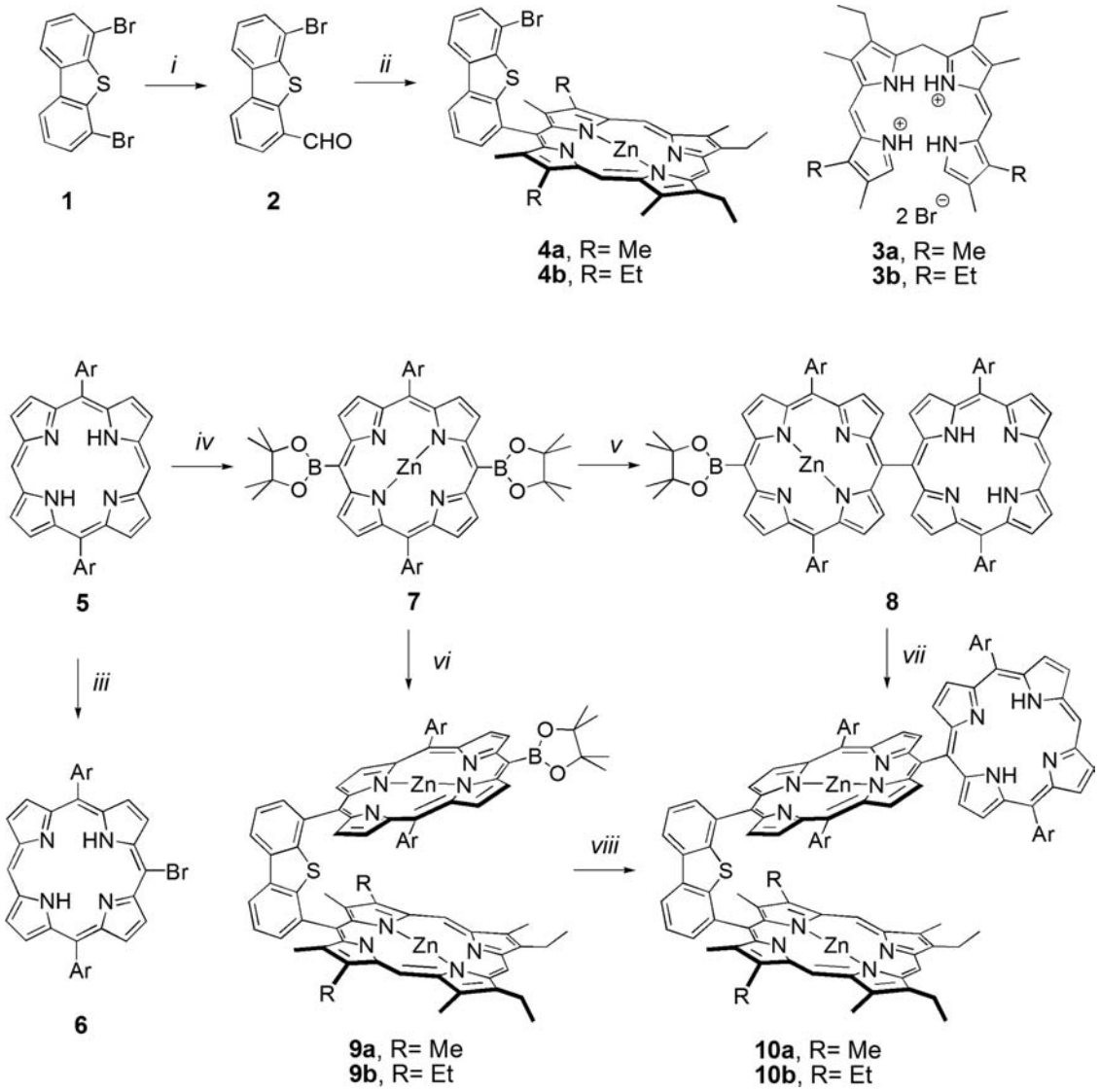

[a](i) (1) PhLi, (2) DMF, (3) H_2O; (ii) p-TSA, (**3a**,**b**), (2) $Zn(OAc)_2$; (iii) (1) NBS; (iv) (1) NBS, (2) $Zn(OAc)_2$, (3) pinacolborane, $PdCl_2(PPh_3)_2$, NEt_3; (v) **6**, $Pd(PPh_3)_4$, Cs_2CO_3, toluene/DMF, 90 °C (5 h); (vi) **4a**,**b**, $Pd(PPh_3)_4$, Cs_2CO_3, toluene/DMF, 90 °C (5 h); (vii) **4b**, $Pd(PPh_3)_4$, Cs_2CO_3, toluene/DMF, 90 °C (14 h); (viii) **6**, $Pd(PPh_3)_4$, Cs_2CO_3, toluene/DMF, 90 °C (14 h).

1H, J = 4.9 Hz, β), 9.03 (d, 1H, J = 4.6 Hz, β), 9.00 (d, 1H, J = 4.7 Hz, β), 8.92 (m, 2H, thiophene), 8.82 (d, 2H, J = 4.7 Hz, β), 8.75 (d, 2H, J = 4.6 Hz, β), 8.52 (d, 1H, J = 4.8 Hz, β), 8.34 (m, 3H, 1 thiophene + 2β), 8.22 (d, 1H, J = 4.8 Hz, β), 8.12−8.01 (m, 5H, 3 thiophene + 2C_6H_4), 7.95 (d, 2H, J = 8.1 Hz, C_6H_4), 7.89 (d, 2H, J = 8.2 Hz, C_6H_4), 7.84 (d, 1H, J = 4.9 Hz, β), 7.75 (d, 2H, J = 4.7 Hz, β), 7.66 (d, 2H, J = 8.2 Hz, C_6H_4), 7.48 (d, 2H, J = 8.3 Hz, C_6H_4), 7.43 (d, 2H, J = 7.6 Hz, C_6H_4), 7.30 (m, 5H, 1β+C_6H_4), 3.94 (q, J = 7.7 Hz, 4H, CH_2), 3.46 (s, 6H, CH_3), 3.36 (s, 6H, CH_3), 2.93 (q, J = 7.7 Hz, 2H, CH_2), 2.86 (q, J = 7.7 Hz, 6H, CH_2), 2.33 (s, 6H, CH_3), 1.74 (t, J = 7.6 Hz, 6H, CH_3), 1.47 (m, masked by water), 1.40 (t, J = 7.6 Hz, 3H, CH_3), 1.39 (t, J = 7.4 Hz, 6H, CH_3), and −2.60 (s, 2H, NH) ppm. ESI HRMS m/z: 1789.5944 (M + H^+), 1789.5856 calcd for $C_{114}H_{93}N_{12}SZn_2$, 1811.5764 [M + Na]$^+$, 1811.5764 calcd for $C_{114}H_{92}N_{12}SNaZn_2$. UV−vis (THF) λ_{max} (log ε) = 411 (5.65), 432 sh (5,12), 455 (5.17), 513 (4.48), 546 (4.42), 562 (4.53), 577 (4.36), 600 (4.05), 647 (3.49) nm.

*Zinc(II) 5-{4-[Zinc(II)(2,8,13,17-tetraethyl-3,7,12,18-tetramethyl)-porphyrin-5-yl]-dibenzothien-6-yl}-[10,20-bis-(4-ethylphenyl)-porphyrin-5-yl]-10,20-bis-(4-ethyl-phenyl)porphyrin (**10b**).* For route A, following the above procedure, 23 mg (44%) of a brownish purple solid was obtained starting from **9b** (43 mg, 0.030 mmol) and **6** (24 mg, 0.040 mmol). For route B, in a Schlenk tube, 4 mL of anhydrous toluene was added under argon on a mixture of **4b** (30 mg, 0.037 mmol), **8** (35 mg, 0.028 mmol), cesium carbonate (22 mg, 0.067 mmol), and $Pd(PPh_3)_4$ (3.3 mg, 0.0030 mmol). A 2 mL portion of anhydrous DMF was added, and the reaction mixture was stirred at 90 °C for 14 h. The solvents were removed, and the residue was redissolved in toluene (50 mL) and stirred with an aqueous saturated NH_4Cl solution (50 mL). The organic layer was separated and washed with water (2 × 60 mL). The solvent was evaporated and purification by column chromatography (silica gel, chloroform/petroleum ether 1/1) followed by preparative size exclusion chromatography (BioRad Bio-Beads SX-1 packed in CH_2Cl_2) afforded the product (28 mg, 55%). ^{1}H NMR (both isomers, 300.16 MHz, CD_2Cl_2): δ 10.30 (s, 2H, *meso*), 9.95 (s, 1H, *meso*), 9.93 (s, 2H, *meso*), 9.92 (s, 1H, *meso*), 9.86 (s, 1H, *meso*), 9.83 (s, 1H, *meso*), 9.46 (m, 1H, β), 9.40 (m, 3H, β), 9.10 (1H, m, β), 9.03 (m, 3H, β), 8.93 (m, 4H, thiophene), 8.76−8.66 (m, 8H, thiophene + β), 8.51 (d, 1H, J = 4.8 Hz, β), 8.50 (d, 1H, J = 4.8 Hz, β), 8.38−8.23 (m, 8H, thiophene + β), 8.08−7.99 (m, 13H, thiophene + β + C_6H_4), 7.88 (m, 4H, C_6H_4), 7.83 (t, 2H, J = 4.8 Hz, β), 7.75 (d, 3H, J = 5.2 Hz, β), 7.64 (m, 4H, C_6H_4), 7.53−7.48 (m,

dx.doi.org/10.1021/ic3026655 | *Inorg. Chem.* 2013, 52, 8360−8368

10H, C_6H_4), 7.37 (m, 10H, β + C_6H_4), 3.93 (m, 8H, CH_2), 3.47 (s, 3H, CH_3), 3.44 (s, 6H, CH_3), 3.40 (s, 3H, CH_3), 3.39 (s, 6H, CH_3), 3.00−2.72 (m, 23H, CH_2+ CH_3), 2.57 (m, 4H, CH_2), 2.30 (s, 3H, CH_3), 1.74 (t, J = 6.9 Hz, 6H, CH_3), 1.72 (t, J = 7.3 Hz, 6H, CH_3), 1.61−1.44 (m, masked by water, CH_3), 1.42−1.36 (m, 21H, CH_3), 1.06 (t, J = 7.4 Hz, 12H, CH_3), −3.42 (s, 1H, NH), and −2.59 (s, 3H, NH) ppm. HR-MALDI-TOF m/z: 1816. 6177 $[M]^{\bullet+}$, 1816.6185 calcd for $C_{116}H_{96}N_{12}SZn_2$. UV−vis (THF) λ_{max} (log ε) = 412 (5.46), 456 (5.01), 513 (4.36), 566 (4.39), 600 (3.96), 648 (3.49) nm.

Instrumentation. ^{1}H NMR spectra were recorded on a Bruker Avance II 300 (300 MHz) or on a Bruker Avance DRX 500 (500 MHz) spectrometer at the "*Plateforme d'Analyse Chimique et de Synthèse Moléculaire de l'Université de Bourgogne (PACSMUB)*"; chemical shifts are expressed in ppm relative to chloroform (7.26 ppm), methylene chloride (5.32 ppm), or THF-d_8 (1.73 and 3.58 ppm). Mass spectra and accurate mass measurements (HR-MS) were obtained on a Bruker Daltonics Ultraflex II spectrometer in the MALDI/TOF reflectron mode using dithranol as a matrix or on a Bruker MicroQTof instrument in ESI mode. Both measurements were performed at the "*Plateforme d'Analyse Chimique et de Synthèse Moléculaire de l'Université de Bourgogne (PACSMUB)*". UV−vis absorption spectra were recorded on a Hewlett-Packard, model 8452A, diode array, or on a Varian Cary model 500 or on a Varian Cary 1 spectrophotometer. The emission spectra were obtained with a Spex Fluorolog 2. Nanosecond temporal decay profiles were measured using a PTI TimeMaster Model TM-3 instrument fitted with a nitrogen laser-pumped dye laser (fwhm ∼1.4 ns). Fluorescence lifetimes were obtained by iterative reconvolution of the instrument response functions with trial mono-, bi-, or triexponential functions and by distribution lifetimes analysis (exponential series method; ESM), using goodness-of-fit metrics to obtain the best decay parameters. These measurements were performed several times in order to have an uncertainty based on the maximum and minimum obtained values. With high quality data, this technique allows reliable and reproducible data down to 100 ps. Nanosecond fluorescence lifetimes at 77 K were obtained with the PTI instrument by placing the sample in 2-MeTHF (2-methyltetrahydrofuran) in an NMR tube and flash freezing it in liquid N_2.

Quantum Yields. S_1 fluorescence quantum yields were measured in triplicate in 2-MeTHF at room temperature on samples prepared under an inert atmosphere (P_{O2} < 25 ppm) in a glovebox. The reference fluorophore was the free base tetraphenylporphyrin, H_2TPP, a common standard for porphyrin spectroscopy,[12] for which Φ_f = 0.11[12a] as different from Φ_f = 0.048 (in deoxygenated benzene) reported by Finikova et al. (See refs 40, 41, 48, and 49 of reference 12b.) The sample and standard concentrations were adjusted to obtain the same absorbance, $A \leq 0.05$, at the 550 nm excitation wavelength, and each absorbance was measured five times for improved precision. The quantum yields listed represent the total emission yields from the integrated areas under the whole of the emission spectra; no attempt was made to try to separate the total emission into separate contributions from the excited free base and zinc porphyrins.

Computations. The structure optimizations were calculated with the Gaussian 09 software,[13] at the Université de Sherbrooke's Mammouth super computer, supported by the Réseau Québécois de Calcul de Haute Performance. The DFT[14−17] was calculated by the B3LYP[18−20] method with 3-21G* basis sets on all atoms.[21−23]

RESULTS AND DISCUSSION

Synthesis. The synthesis of **10a,b** proceeds in several steps from the dibenzothiophene, which is first brominated in the known 4,6-dibromodibenzothiophene (**1**)[7] (Scheme 1).

Selective monolithiation of **1** with PhLi in the presence of DMF, followed by hydrolysis of the resulting imidate salt, provides the 4-bromo-6-formyldibenzothiophene compound **2** in 78% yield. The acid-catalyzed condensation of **2** with 1 equiv of a,c-biladienes **3a,b**[9] followed by metalation gives the zincated porphyrins **4a,b** in modest yields (∼25%). The monobromination of **5** at the *meso*-position using *N*-bromosuccinimide (NBS) yields compound **6**, meanwhile using 2 equiv of NBS generates the intermediate dibromoporphyrin.[10,11] The latter is then metalated with $Zn(OAc)_2{\cdot}2H_2O$ and converted into the bisborylated zinc(II)porphyrin **7** with pinacolborane under Masuda conditions.[24] These three successive steps provide **7** in 77% overall yield. This versatile metalloporphyrin is then suitable for Suzuki reactions and can be used for the synthesis of DPS-based trimers **10a,b** in two pathways depending on the sequence of the reactants **4a,b** versus **6**. The metal-catalyzed stepwise functionalization of porphyrins at *meso* and β positions has recently emerged as a promising tool for the direct carbon−carbon bond formation between porphyrinic units.[25] After a rapid survey of catalysis conditions using $Pd(PPh_3)_4$ as the catalyst, the Suzuki couplings are performed in a toluene−DMF medium and Cs_2CO_3 as base and the reagent ratios and reaction times were optimized.[25c,h,26] The cross coupling between **7** and **4a,b** provides the cofacial bisporphyrins **9a,b** in yields of ∼65% similar to that reported by Nocera and co-workers for DPS-based cofacial bis(porphyrins).[27] Dimer **8** was isolated in 62% yield from the reaction between **7** and **6**. The subsequent Suzuki reaction between dimers **9a,b** and **6** yields triads **10a,b** in 44−48% but requires a longer reaction time, and higher ratio free base/dimer lowers the byproduct formation. Compound **10b** was also alternatively synthesized from the cross coupling of **8** with **4b**. Traces of a fully metalated triad were also detected with **10b** after silica gel chromatography. This mixture was submitted to size exclusion chromatography, and a very low amount of pure triad **10b** was obtained after several purification steps. The presence of the fully metalated trimer makes this route unfavorable. The latter compound was not investigated.

In the absence of X-ray data, DFT (B3LYP) was used to address the structures of **10a,b** and **9a,b**. It is assumed that **10a** and **9a** are representative examples. The optimized structure of **10a** (Figure 2) exhibits the expected slipped cofacial geometry for the octaalkyl zinc(II)porphyrin/diaryl zinc(II)porphyrin

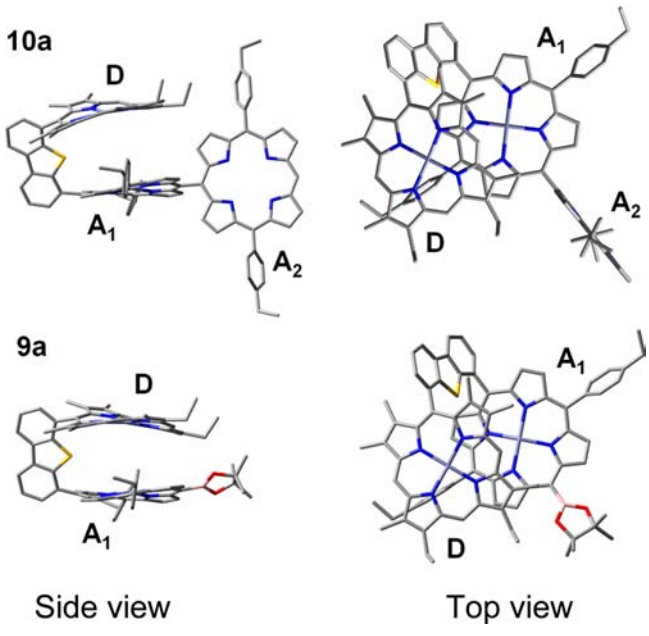

Figure 2. Views of the optimized geometry (DFT: B3LYP) of **10a** (top) and **9a** (bottom).

dx.doi.org/10.1021/ic3026655 | *Inorg. Chem.* 2013, 52, 8360−8368

unit, blocked by the free base macrocycle. Steric hindrance prevents the free base from being placed between the two central Et groups. The dihedral angle formed by the diaryl zinc(II)porphyrin and free base average planes is 84.2°. This angle is calculated to be similar to 82.3° for **8**. The angle formed by the atom surrounding the $C_{meso}-C_{meso}$ bond (i.e., $C_2C_{meso}-C_{meso}C_2$) is 88.3° resembling that of dimer **8** (89.2°). The latter feature indicates that electronic communication between $\mathbf{A_1}$ and $\mathbf{A_2}$ via conjugation is minimal. The other characteristic features, such as the computed $C_{meso}\cdots C_{meso}$ separations between **D** and $\mathbf{A_1}$ (6.12 and 6.05 Å), the angles formed by the average planes of **D** and $\mathbf{A_1}$ (12.9° and 6.9°), and the angle formed by the average $C_{meso}\cdots Z\cdots C_{meso}$ axis of **D** and $\mathbf{A_1}$ (22.4° and 25.5° for **10a** and **9a**, respectively), indicate a strong structure similarity making **9a,b** appropriate for comparison with **10a,b**.

From a photophysical standpoint, the choice of these systems is based on several important considerations. First, the dibenzothiophene bridge (DPS) is selected because of its long resulting $C_{meso}\cdots C_{meso}$ separation in the cofacial bis porphyrin skeleton (6.30 Å) so that the fluorescence lifetime, τ_F, of **D** (octaalkyl zinc(II)porphyrin) in the presence of an acceptor is still long enough to obtain the maximum precision possible on the measurements.[28] Second, the fluorescence lifetime in the absence of the acceptor, $\tau_F(D)^o$, is the same for the bromo-DPS-octaalkyl zinc(II)porphyrin (**4a,b**, Scheme 1) as for the DPS-bis(octaalkyl zinc(II)porphyrin).[28] This means that the rates for intersystem crossing, k_{ISC}, and internal conversion, k_{IC}, are not affected when a group is placed the position of chromophore $\mathbf{A_1}$. This is important because this allows us to use **4a,b** as an adequate standard for $\tau_F(D)^o$ for accurate extraction of the rate for energy transfer (k_{ET}) described below. Third, the use of octaalkyl zinc(II)porphyrin, diaryl zinc(II)porphyrin, and free base diarylporphyrin promotes only energy transfer and no electron transfer occurs.[2] Finally, because of the possible dynamic rotation about the DPS-(diaryl zinc(II)porphyrin) single bond, this study was also performed in frozen media at 77 K to ensure that only the lowest energy conformation is analyzed (see section on the fluxionality of **9b** and **10b**). This effect was recently demonstrated for a series of cofacial dyads similar to **9a,b** where a linear relationship is observed at 77 K between k_{ET} and the gap of the 0−0 peak positions of the absorption or fluorescence of the donor and acceptor but not at 298 K.[29]

The indicated roles **D**, $\mathbf{A_1}$, and $\mathbf{A_2}$ in Figure 1 for **4a**, **9a,b**, and **10a,b** are assigned from the position of the 0−0 peaks observed in the absorption and fluorescence spectra, associated with the chromophores octaalkyl zinc(II)porphyrin (577 and ∼580 nm, higher energy), diaryl zinc(II)porphyrin (∼600 and 606 nm, intermediate energy), and diarylporphyrin free base, respectively (648 and 654 nm, lower energy; Figure 3 for **4a**, **9a**, and **10a** at 298 K, see SI for **8**, **9b**, and **10b** at 298 K and all 77 K spectra; Figures S32−S45). Tables 1 and 2 provide the absorption and fluorescence data.

The excitation spectra monitored all across the fluorescence bands superpose well the absorption (see Figures S32−S45 in the SI) meaning that the S_1 energy transfers occur efficiently for all chromophores. As a result of the efficient energy transfers, the fluorescence intensity of **D** and $\mathbf{A_1}$ is expectedly weak as clearly illustrated in Figure 3. The $k_{ET}(S_1)$ values are extracted from $k_{ET} = (1/\tau_F) - (1/\tau_F^o)$ where τ_F and τ_F^o are the fluorescence lifetimes of the donor, respectively, in the presence and absence of an energy acceptor.[2] The τ_F^o, τ_F, and k_{ET} data

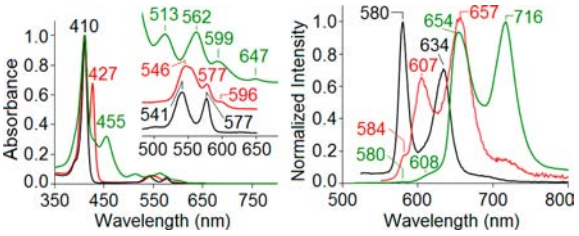

Figure 3. Absorption (left) and fluorescence (right) of **4a** (black), **9a** (red), and **10a** (green) in 2-MeTHF at 298 K. Inset shows expansion of the Q-region.

Table 1. Absorption Data for 4a,b−10a,b in 2-MeTHF

	λ_{max} nm (at 298 K)		λ_{max} /nm (at 77 K)	
compd	Soret region	Q bands	Soret region	Q bands
4a	410	541, 577	410	532, 572
4b	412	541, 577		
5	405	501, 535, 576, 633		
8	418, 447	513, 559, 590, 649	424, 450	516, 560, 588, 644
9a	410, 427	546, 577, 596	412, 430	542, 555, 562, 574, 600
9b	411, 426	546, 577, 602	414, 430	542, 555, 562, 575, 599
10a	411, 455	513, 546, 562, 577, 600, 647	412, 430, 458	514, 540, 566, 574, 582
10b	412, 456	513, 566, 600, 648	414, 429, 458	514, 542, 562, 583

Table 2. Fluorescence Data for 4a,b−10a,b (2-MeTHF, Uncertainties of the λ_{max} ±1 nm)

	298K				77 K	
compd	λ_{exc}/ nm	λ_{max}/ nm	τ_F/ns	Φ_F[a]	λ_{max}/nm	τ_F/ns
4a	505	580, 634	1.7	0.021	576, 632, 702, 785	1.92
4b	525	581, 633, 696	*b*	*b*	*b*	*b*
5	505	644, 712	10.1	0.075		
8	505	655, 718	10.4	0.093	599, 643, 655 sh, 684, 702 sh, 713	2.34
9a	505	584, 607, 657	2.2[c]	0.027	575, 603, 661, 768	0.181, 3.02
9b	505	584, 606, 655	0.27, 2.1	0.031	576, 603, 662, 770	0.195, 3.39
10a	495	654, 716	*b*	*b*	576, 615, 644, 655 sh, 683, 705 sh, 713	0.145, 11.6[d]
10b	495	654, 716	*b*	*b*	574, 618, 643, 655 sh, 683, 703 sh, 713	0.155, 11.6[d]

[a]The Φ_F values were measured against H_2TPP ($\Phi_F = 0.11$), but a later report indicated that the value of H_2TPP is 0.048 (in deoxygenated benzene).[12b] These values should be taken with caution. [b]Not measured. [c]A value of 0.25 ns was observed, but the relative intensity is very weak. [d]A ∼2 ns component is also noted but could not be accurately evaluated. It is likely due to the zinc(II)porphyrin chromophore $\mathbf{A_1}$.

are compared in Table 3. The decays along with the ESM analyses for **9a,b** and **10a,b** are presented in Figures S46−S48 (SI). Because the fluorescence lifetime of $\mathbf{A_1}$ could not be evaluated in this work (see footnote in Table 3), the energy

dx.doi.org/10.1021/ic3026655 | Inorg. Chem. 2013, 52, 8360−8368

Table 3. τ_F and τ_F^o Data in 2-MeTHF at 77 K

compd	chromophore	τ_F/ns[a]	λ/nm[b]	$k_{ET}(S_1) \times 10^{-9}/s^{-1}$
4a	**D**	1.9 ± 0.1	575	
8	$\mathbf{A_1}$		584	
	$\mathbf{A_2}$	10.9 ± 0.1	640	
9a	**D**	0.181 ± 0.013	565	5.0
	$\mathbf{A_1}$	3.02 ± 0.04	593	
9b	**D**	0.195 ± 0.025	575	4.7
	$\mathbf{A_1}$	3.39 ± 0.33	600	
10a	**D**	0.145 ± 0.050	575	6.4
	$\mathbf{A_1}$	*c*	600	
	$\mathbf{A_2}$	11.6 ± 0.2	640	
10b	**D**	0.155 ± 0.050	575	5.9
	$\mathbf{A_1}$	*c*	605	
	$\mathbf{A_2}$	11.6 ± 0.2	654	

[a]The τ_F values are measured several times, and the uncertainties are based on three different measurements using highly accurate ESM analyses. The data were highly reproducible. The uncertainties are from the largest and smallest measured values. [b]Monitoring wavelength. [c]The decays exhibit components of both **D** and $\mathbf{A_2}$, but a component of ~2 ns was also necessary to obtain the best fits, hence accurately extracting the short-lived components at low wavelength and the long-lived one at high wavelengths. This component is most likely due to $\mathbf{A_1}$, but its exact value is unsure.

transfer process $\mathbf{A_1}^* \rightarrow \mathbf{A_2}$ is not investigated (i.e., the $k_{ET}(S_1)$ could not be measured reliably).

The τ_F and τ_F^o data (Table 3) were tested for consistencies by comparing the τ_F^o data for **4a** with those previously reported for **11** and **12** (Figure 4). Indeed, the data compare favorably. Similarly, $k_{ET}(S_1)$ for **9a,b** (5.0×10^9 and 4.7×10^9 s^{-1}) also compares well with that for **13** (Figure 4; 4.6×10^9 s^{-1}).[28] The similarity of the photophysical data between **4a** and **4b**, and **9a** and **9b** indicates that the R group (Me vs Et) has a minimal effect, if any, on τ_F and $k_{ET}(S_1)$. It is noteworthy that $\tau_F(\mathbf{A_2})$ increases only very slightly going from **8** (10.9 ± 0.1 ns) to **10a,b**, (both 11.6 ± 0.2 ns) indicating that the rate for internal conversion, k_{ic}, is not increased upon the incorporation of $\mathbf{A_2}$ in the trimers and has no major effect. In other words, k_{ic} has no role on the change in the τ_F upon the incorporation of the $\mathbf{A_2}$ chromophore in the **10a,b** trimers.

The $k_{ET}(S_1)$ values for **10a,b** are systematically larger than that for **9a,b** indicating the presence of an extra deactivation pathway, and again cannot be associated with any additional nonradiative deactivation processes. Their amplitude (~6.2×10^9 s^{-1}) is similar to that recently reported for compound **14** (11×10^9 s^{-1}; Figure 4) using time-resolved femtosecond transient absorption spectroscopy.[30] The larger global $k_{ET}(S_1)$ value for **14** over **10a,b** is fully consistent with the shorter $\mathbf{D}\cdots\mathbf{A_1}$ separation for the former (distance $C_{meso}\cdots C_{meso}$ = 4.98 Å for anthracenyl, 6.30 Å for DPS).[28] Consequently, **D** is closer to both $\mathbf{A_1}$ and $\mathbf{A_2}$. Indeed, Förster's theory that states $k_{ET}(S_1) \propto (1/r^6)$.[32]

The subtraction of $k_{ET}(S_1)$ of **9a,b** from **10a,b** gives $k_{ET}(S_1)$ the through space process $\mathbf{D}^* \rightarrow \mathbf{A_2}$ (Figure 1). The resulting k_{ET} values are 1.4×10^9 and 1.2×10^9 s^{-1}, with 39% and 54% uncertainties, for **10a** and **10b**, respectively. Assuming $k_{ET}(S_1)$ is still independent of R (R = Me or Et), then $k_{ET}(S_1)$ is ~1×10^9 s^{-1}, which represents ~15% of the total value found for **D** in **10a,b** (i.e., ~6×10^9). This lower value is an expected consequence of the longer center-to-center $\mathbf{D}\cdots\mathbf{A_2}$ distance over that for $\mathbf{D}\cdots\mathbf{A_1}$,[28] as the Förster theory predicts.[31] Moreover,

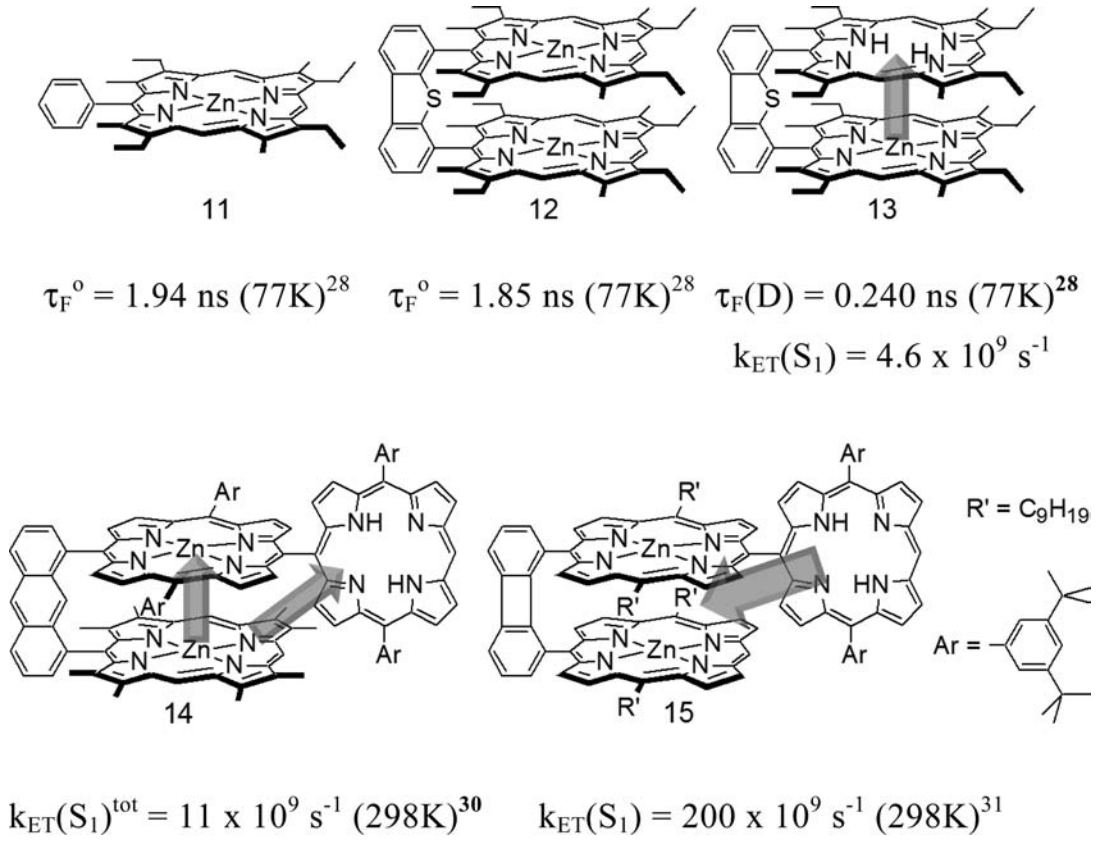

Figure 4. Structures of compounds **11**–**15**. The arrows indicate the directions of the S_1 energy transfer.

dx.doi.org/10.1021/ic3026655 | *Inorg. Chem.* 2013, 52, 8360–8368

the relative orientation of the transition moment vectors are also unfavorable for efficient energy transfer (near the right angle).[32] Despite the structural resemblance between **10a,b** and **15**[31] (Figure 4), the k_{ET} values differ greatly ($\sim 6 \times 10^9$ vs 200×10^9 s^{-1}). A previously proposed and reasonable explanation for this is the presence of a large MO mixing occurring in **15** notably between **D** and $\mathbf{A_2}$ due to very close proximity.[33]

Although the $\mathbf{A_1}^* \rightarrow \mathbf{A_2}$ energy transfer process could not be reliably investigated in this work, ultimately the $\mathbf{A_2}$ acceptor is the final site prior to most of the observed fluorescence with only a very weak signal associated with $\mathbf{A_1}$ (green trace in Figure 3; right). Because the $k_{ET}(S_1)$ is the same for **9a,b** and **13**, the $k_{ET}(S_1)$ for this $\mathbf{A_1}^* \rightarrow \mathbf{A_2}$ process in **10a,b** must be larger than that for the $\mathbf{D}^* \rightarrow \mathbf{A_1}$ process as it is not the limiting factor. To the best of our knowledge, there is no other work that reports a donor–acceptor system, here **D** and $\mathbf{A_2}$ (i.e., not identical chromophores), linked by conjugated bonds only, normally favored through bond energy transfers, but occurring exclusively via through space energy transfer.

■ ASSOCIATED CONTENT

Supporting Information

Characterization spectra, all photophysical spectra and fluorescence decays at 298 and 77 K, and computer modeling of compound **9b**. This material is available free of charge via the Internet at http://pubs.acs.org.

■ AUTHOR INFORMATION

Corresponding Author

*E-mail: roger.guilard@u-bourgogne.fr (R.G.); Pierre.Harvey@USherbrooke.ca (P.D.H.). Phone: 33 380 39 61 11 (R.G.); 001-819-821-7092 (P.D.H.). Fax: 33 380 39 61 17 (R.G.); 001-819-821-8017 (P.D.H.).

Notes

The authors declare no competing financial interest.

[§]On leave from the Chemistry Department, Assiut University, Assiut, Egypt.

■ ACKNOWLEDGMENTS

P.D.H. thanks the Natural Sciences and Engineering Research Council of Canada, NSERC, and the Fonds Québécois de la Recherche sur la Nature et les Technologies, FQRNT, and the Agence Nationale de la Recherche, ANR, for the grant of a Research Chair of Excellence for P.D.H.. R.G. thanks the CNRS (Centre National de la Recherche Scientifique) and the Université de Bourgogne for funding.

■ REFERENCES

(1) *Light-Harvesting Antennas in Photosynthesis in Advances in Photosynthesis and Respiration*; Green, B. R., Parson, W. W., Eds.; Kluwer: Dordrecht, 2003; Vol *13*.

(2) (a) Harvey, P. D.; Stern, C.; Guilard, R. *Handbook of Porphyrin Science with Applications to Chemistry, Physics, Materials Science, Engineering, Biology and Medicine*; Kadish, K. M., Smith, K. M., Guilard, R.; Eds.; World Scientific Publishing: Singapore, 2011; Vol. *11*, pp 1–177. (b) Harvey, P. D. *The Porphyrin Handbook*; Kadish, K. M., Smith, K. M., Guilard, R., Eds.; Academic Press: San Diego, 2003; Vol. *18*, Chapter 113.

(3) (a) Baranoff, E.; Collin, J.-P.; Flamigni, L.; Sauvage, J.-P. *Chem. Soc. Rev.* **2004**, *33*, 147–155. (b) Yang, J.; Yoon, M.-C.; Yoo, H.; Kim, P.; Kim, D. *Chem. Soc. Rev.* **2012**, *41*, 4808–4826. (c) Panda, M. K.; Ladomenou, K.; Coutsolelos, A. G. *Coord. Chem. Rev.* **2012**, *256*, 2601–2627. (d) Yedukondalu, M.; Ravikanth, M. *J. Chem. Sci.* **2011**, *123*, 201–214. (e) Harvey, P. D.; Stern, C.; Gros, C. P.; Guilard, R. *J. Porphyrins Phthalocyanines* **2010**, *14*, 55–63. (f) Otsuki, J. *J Porphyrins Phthalocyanines* **2009**, *13*, 1069–1081. (g) Boyle, N. M.; Rochford, J.; Pryce, M. T. *Coord. Chem. Rev.* **2010**, *254*, 77–102. (h) Aratani, N.; Kim, D.; Osuka, A. *Acc. Chem. Res.* **2009**, *42*, 1922–1934. (i) Albinsson, B.; Martensson, J. *J. Photochem. Photobiol., C* **2008**, *9*, 138–155.

(4) In *Multiporphyrin Arrays, Fundamentals and Applications*; Kim, D., Ed.; Pas Stanford: Singapore, 2012.

(5) Sessler, J. L.; Wang, B.; Harriman, A. *J. Am. Chem. Soc.* **1995**, *117*, 704–714.

(6) Cho, H. S.; Jeong, D. H.; Yoon, M.-C.; Kim, Y. H.; Kim, Y.-R.; Kim, D.; Jeoung, S. C.; Kim, S. K.; Aratani, N.; Shinmori, H.; Osuka, A. *J. Phys. Chem. A* **2001**, *105*, 4200–4210.

(7) Chantson, J. T.; Lotz, S.; Ichharam, V. *New J. Chem.* **2003**, *27*, 1735–1740.

(8) Laha, J. K.; Dhanalekshmi, S.; Taniguchi, M.; Ambroise, A.; Lindsey, J. S. *Org. Process Res. Dev.* **2003**, *7*, 799–812.

(9) Johnson, A. W.; Kay, I. T. *J. Chem. Soc.* **1961**, 2418–2423.

(10) DiMagno, S. G.; Lin, V. S. Y; Therien, M. J. *J. Org. Chem.* **1993**, *58*, 5983–5993.

(11) Yu, L.; Muthukumaran, K.; Sazanovich, I. V.; Kirmaier, C.; Hindin, E.; Diers, J. R.; Boyle, P. D.; Bocian, D. F.; Holten, D.; Lindsey, J. S. *Inorg. Chem.* **2003**, *42*, 6629–6647.

(12) (a) Seybold, P. G.; Gouterman, M. *J. Mol. Spectrosc.* **1969**, *31*, 1–13. (b) Finikova, O. S.; Troxler, T.; Senes, A.; DeGrado, W. F.; Hochstrasser, R. M.; Vinogradov, S. A. *J. Phys. Chem. A* **2007**, *111*, 6977–6990.

(13) Gaussian, Inc., 340 Quinnipiac St., Bldg. 40, Wallingford, CT 06492.

(14) Hohenberg, P.; Kohn, W. *Phys. Rev. B* **1964**, *136*, 864–871.

(15) Kohn, W.; Sham, L. J. *Phys. Rev. A* **1965**, *140*, 1133–1138.

(16) *The Challenge of d and f Electrons*; Salahub, D. R., Zerner, M. C., Eds.; American Chemical Society: Washington, DC, 1989.

(17) Parr, R. G.; Yang, W., *Density-Functional Theory of Atoms and Molecules*, Oxford University Press: Oxford, 1989.

(18) Becke, A. D. *J. Chem. Phys.* **1993**, *98*, 5648–5652.

(19) Lee, C.; Yang, W.; Parr, R. G. *Phys. Rev. B: Condens. Matter Mater. Phys.* **1988**, 785–789.

(20) Miehlich, B.; Savin, A.; Stoll, H.; Preuss, H. *Chem. Phys. Lett.* **1989**, *157*, 200–206.

(21) Binkley, J. S.; Pople, J. A.; Hehre, W. J. *J. Am. Chem. Soc.* **1980**, *102*, 939–947.

(22) Gordon, M. S.; Binkley, J. S.; Pople, J. A.; Pietro, W. J.; Hehre, W. J. *J. Am. Chem. Soc.* **1982**, *104*, 2797–2803.

(23) Pietro, W. J.; Francl, M. M.; Hehre, W. J.; Defrees, D. J.; Pople, J. A.; Binkley, J. S. *J. Am. Chem. Soc.* **1982**, *104*, 5039–5048.

(24) (a) Murata, M.; Watanabe, S.; Masuda, Y. *J. Org. Chem.* **1997**, *62*, 6458–6459. (b) Hyslop, A. G.; Kellett, M. A.; Iovine, P. M.; Therien, M. J. *J. Am. Chem. Soc.* **1998**, *120*, 12676–12677.

(25) (a) Song, J.; Aratani, N.; Kim, P.; Kim, D.; Shinokubo, H.; Osuka, A. *Angew. Chem., Int. Ed.* **2010**, *49*, 3617–3620. (b) Nakamura, Y.; Jang, S. Y.; Tanaka, T.; Aratani, N.; Lim, J. M.; Kim, K. S.; Kim, D.; Osuka, A. *Chem.—Eur. J.* **2008**, *14*, 8279–8289. (c) Aratani, N.; Osuka, A. *Org. Lett.* **2001**, *3*, 4213–4216. (d) Deng, Y.; Chang, C. K.; Nocera, D. G. *Angew. Chem., Int. Ed.* **2000**, *39*, 1066–1067. (e) Bringmann, G.; Gulder, T. A. M.; Gehrke, T. H.; Kupfer, T.; Radacki, K.; Braunschweig, H.; Heckmann, A.; Lambert, C. *J. Am. Chem. Soc.* **2008**, *130*, 17812–17825. (f) Götz, D. C. G.; Bruhn, T.; Senge, M. O.; Bringmann, G. *J. Org. Chem.* **2009**, *74*, 8005–8020. (g) Wu, C.-A.; Chiu, C.-L.; Mai, C.-M.; Lin, Y.-S.; Yeh, C.-Y. *Chem.—Eur. J.* **2009**, *15*, 4534–4537. (h) Cheng, F.; Zhang, S.; Adronov, A.; Echegoyen, L.; Diederich, F. *Chem.—Eur. J.* **2006**, *12*, 6062–6070.

(26) Filatov, M. A.; Guilard, R.; Harvey, P. D. *Org. Lett.* **2010**, *12*, 196–199.

(27) Chng, L. L.; Chang, C. J.; Nocera, D. G. *J. Org. Chem.* **2003**, *68*, 4075–4078.

(28) Faure, S.; Stern, C.; Guilard, R.; Harvey, P. D. *J. Am. Chem. Soc.* **2004**, *126*, 1253–1261.

(29) Camus, J.-M.; Aly, S. M.; Stern, C.; Guilard, R.; Harvey, P. D. *Chem. Commun.* **2011**, *47*, 8817−8819.
(30) Harvey, P. D.; Langlois, A.; Filatov, M.; Fortin, D.; Ohkubo, K.; Fukuzumi, S.; Guilard, R. *J. Porphyrins Phthalocyanines* **2012**, *16*, 685−694.
(31) Filatov, M. A.; Laquai, F.; Fortin, D.; Guilard, R.; Harvey, P. D. *Chem. Commun.* **2010**, *48*, 9176−9178.
(32) Forster, T. *Ann. Phys.* **1948**, *2*, 55−75.
(33) (a) Uetomo, A.; Kozaki, M.; Suzuki, S.; Yamanaka, K.; Ito, O.; Okada, K. *J. Am. Chem. Soc.* **2011**, *133*, 13276−13279. (b) Tsubaki, K.; Takaishi, K.; Sue, D.; Matsuda, K.; Kanemitsu, Y.; Kawabata, T. *J. Org. Chem.* **2008**, *73*, 4279−4282. (c) Montes, V. A.; Perez-Bolivar, C.; Agarwal, N.; Shinar, J.; Anzenbacher, P., Jr. *J. Am. Chem. Soc.* **2006**, *128*, 12436−12438. (d) Miller, M. A.; Lammi, R. K.; Prathapan, S.; Holten, D.; Lindsey, J. S. *J. Org. Chem.* **2000**, *65*, 6634−6649.